Chiral topological excitonic insulator in semiconductor quantum wells

Ningning Hao,[1,2] Ping Zhang,[2,3,*] Jian Li,[1] Zhigang Wang,[2] Wei Zhang,[2] and Yupeng Wang[1]

[1]*Institute of Physics, Chinese Academy of Sciences, Beijing 100190, People's Republic of China*

[2]*LCP, Institute of Applied Physics and Computational Mathematics, P.O. Box 8009, Beijing 100088, People's Republic of China*

[3]*Center for Applied Physics and Technology, Peking University, Beijing 100871, People's Republic of China*

We present a scheme to realize the chiral topological excitonic insulator in semiconductor heterostructures which can be experimentally fabricated with a coupled quantum well adjacent to two ferromagnetic insulating films. The different mean-field chiral topological orders, which are due to the change in the directions of the magnetization of the ferromagnetic films, can be characterized by the Thouless, Kohmoto, Nightingale, and Nijs numbers in the bulk system as well as by the winding numbers of the gapless states in the edged system. Furthermore, we propose an experimental scheme to detect the emergence of the chiral gapless edge state and distinguish different chiral topological orders by measuring the thermal conductance.

I. INTRODUCTION

The search for new phases of quantum matter is one of the essential topics in condensed-matter physics. Chiral topological band insulators (TBIs) are such a type that has been attracting a lot of interest both theoretically and experimentally. Although like trivial insulators in the sense that TBIs have a band gap in the bulk, they are fundamentally distinguished from trivial ones by their having gapless modes on the boundaries. These gapless modes are robust under perturbations and cannot be gapped without going through a quantum phase transition. In the case of time-reversal symmetry (TRS) breaking, a well-known TBI system is the Haldane's model which is a minimal model to illustrate quantum anomalous Hall effect (QAHE).[1] The QAHE topological phase is characterized by the Thouless, Kohmoto, Nightingale, and Nijs (TKNN) number[2] of the first Chern class of a U(1) principal fiber bundle on a torus in the bulk system or the winding number of Halperin's edge-state theory[3,4] on the boundary of the system. The coherence of the two different kinds of numbers is guaranteed by the bulk-edge correspondence. Since the rigorously prerequisite magnetic field in Haldane's model is difficult to realize in experiment, recently, there are some new proposals[5] to realize QAHE based on single-particle picture.

In analogy with QAHE in single-particle picture, the superconductors in TRS broken (p_x+ip_y) weak pairing state in two dimensions with a fully stable bulk gap opened by electron-electron interaction can also have chiral topological order.[6] The edge states of the chiral superconductor have half of the degrees of freedom compared to QAHE states due to the particle-hole symmetry (PHS) and are called Majorana edge sates. In the spirit of analogy with superconductor, a natural and important issue is how to get chiral topological excitonic insulator (TEI), which is addressed in this paper.

In this paper, we consider an independently gated double-quantum-well structure separated by a spacer as shown in Fig. 1(a). The ferromagnetic insulating films are introduced to break TRS by inducing an effective Zeeman splitting in the two-dimensional electron (hole) gas [2DE(H)G]. The magnetization is perpendicular to the two-dimensional layer.

Note that the orbital effect of the ferromagnetic films to the 2DE(H)G can be neglected due to the local exchange interaction on the interface. An electron-hole fluid is created by modulating the voltages so that the Zeeman-split upper branch of the heavy-hole bands in 2DHG layer can move above the Zeeman-split lower branch of the electron bands in 2DEG layer. This procedure results in spatially separated but strongly interacting electron and hole fluids if the two layers are close enough. The external electric field produced by the bias voltages and the intrinsic electric field due to doping in the process of fabricating quantum wells can enhance the structural inversion asymmetry and induce the tunable Rashba spin-orbit (SO) interaction.[7–10] Recall that due to the strong SO coupling and noncentrosymmeytic property,[11] the broken parity of the order parameter is the prerequisite condition of the chiral superconductor. In analogy with chiral superconductor, we demonstrate that the chiral TEI can occur when the Rashba SO interaction is strong enough with respect to the amplitude of the excitonic order parameter (EOP). Generally the Rashba SO interaction strength can be influenced by carrier density, gated voltages, material of quantum wells, etc.[12–14] In InAs heterostructures, for instance, this quantity can be electrically tuned to be as large as $\alpha \approx 50$ meV Å.[15] Due to the missing PHS, the edge states of chiral TEI in the present system are not Majorana fermions. The implication of these gapless edge states for experimental observations is also discussed in this paper.

II. MODEL AND HAMILTONIAN

We start with an effective electron/hole semiconductor bilayer system confined in the x-y plane. Here for the hole layer only the heavy-hole bands are occupied as in typical experiments while the light-hole bands are empty and are therefore not taken into account in our model. With keeping in mind that around the Γ point, the Rashba SO interaction in conventional semiconductor heterostructures has the familiar expression $\alpha(k_y\sigma_x-k_x\sigma_y)$ for electrons and $i\beta(k_-^3\sigma_+-k_+^3\sigma_-)$ for heavy holes, the resultant tight-binding Hamiltonian for the present bilayer system is $\mathcal{H}=\Sigma_p(\mathcal{H}_{kin}^{(p)}+\mathcal{H}_R^{(p)})+\mathcal{H}_{int}^{(e-h)} \equiv \mathcal{H}_0+\mathcal{H}_{int}^{(e-h)}$,
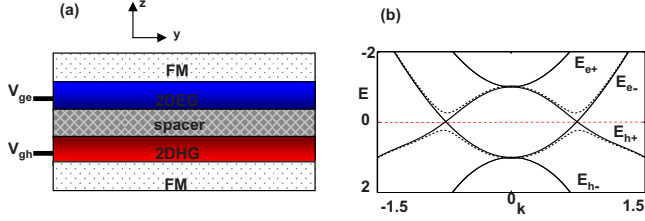
FIG. 1. (Color online) (a) Schematic structure of semiconductor quantum wells system that holds chiral TEI. The external gates ($V_{ge(h)}$) can independently tune the chemical potential $\mu_{e(h)}$ to obtain the electron and heavy-hole layer. The ferromagnetic insulating films support effective exchange fields (V_e, V_h). (b) The energy spectrum of the electron/hole bilayer system near the Fermi energy $E_F \approx 0$. Here the solid lines denote noninteracting single-particle energy spectrum $E_{e(h)\pm}$ while the dashed lines denote the exciton energy spectrum with an obvious mean-field gap opened. We take $t_e = t_h = 1$, $\mu_e = \mu_h = -4$, $(V_e, V_h) = (1,1)$, $\alpha = 0.5$, and $\beta = 0.5$.

$$\mathcal{H}_{kin}^{(p)} = \sum_{\langle i,j\rangle,\sigma} (-t_p - \mu_p \delta_{ij}) p_{i,\sigma}^\dagger p_{j,\sigma} + \sum_{j,\sigma,\sigma'} V_p \tau_p (s_z)_{\sigma,\sigma'} p_{j,\sigma'}^\dagger p_{j,\sigma'},$$

$$\mathcal{H}_R^{(e)} = \frac{1}{2}\alpha \left[\sum_j (e_{j,\uparrow}^\dagger e_{j+\delta x,\downarrow} - e_{j,\uparrow}^\dagger e_{j-\delta x,\downarrow}) - i\sum_j (e_{j,\uparrow}^\dagger e_{j+\delta y,\downarrow} - e_{j,\uparrow}^\dagger e_{j-\delta y,\downarrow}) \right] + \text{H.c.},$$

$$\mathcal{H}_R^{(h)} = \frac{i}{2}\beta \left[\sum_j (h_{j,\Uparrow}^\dagger h_{j+2\delta x,\Downarrow} - h_{j,\Uparrow}^\dagger h_{j-2\delta x,\Downarrow}) + i\sum_j (h_{j,\Uparrow}^\dagger h_{j+2\delta y,\Downarrow} - h_{j,\Uparrow}^\dagger h_{j-2\delta y,\Downarrow}) + 3(1-i)\sum_j (h_{j,\Uparrow}^\dagger h_{j-\delta x+\delta y,\Downarrow} - h_{j,\Uparrow}^\dagger h_{j+\delta x-\delta y,\Downarrow}) + 3(1+i)\sum_j (h_{j,\Uparrow}^\dagger h_{j-\delta x-\delta y,\Downarrow} - h_{j,\Uparrow}^\dagger h_{j+\delta x+\delta y,\Downarrow}) + 4\sum_j (h_{j,\Uparrow}^\dagger h_{j+\delta x,\Downarrow} - h_{j,\Uparrow}^\dagger h_{j-\delta x,\Downarrow}) + 4i\sum_j (h_{j,\Uparrow}^\dagger h_{j+\delta y,\Downarrow} - h_{j,\Uparrow}^\dagger h_{j-\delta y,\Downarrow}) \right] + \text{H.c.},$$

$$\mathcal{H}_{int}^{(e-h)} = -\frac{1}{2}\sum_{i,j,\sigma,\sigma'} U_{i,j}^{(eh)}(d) e_{i\sigma}^\dagger h_{j\sigma}^\dagger h_{j\sigma'} e_{i\sigma}. \quad (1)$$

Here t_p denotes the nearest-neighbor hopping amplitude while μ_p represents the chemical potential in electron ($p = e$) or heavy-hole ($p = h$) layer. s_z is the z component of the Pauli matrices and $V_p \tau_p$ is the effective Zeeman splitting ($\tau_e = 1$ for electron layer and $\tau_h = -1$ for hole layer). $p_{j,\sigma}$ is the fermion annihilation operator at lattice site j with spin $\pm 1/2 (\uparrow, \downarrow)$ for $p = e$ and spin $\pm 3/2 (\Uparrow, \Downarrow)$ for $p = h$. $\alpha(\beta)$ is the Rashba SO interaction strength in the electron (heavy-hole) layer. $\delta x (\delta y)$ is the square-lattice spacing along the $x(y)$ direction. In the interaction term, $U_{i,j}^{(eh)}(d) = e^2/\varepsilon \sqrt{|\vec{R}_{i,e} - \vec{R}_{j,h}|^2 + d^2}$, where ε is the dielectric constant of the spacer and d is the interlayer distance. We only consider the interaction correlative to exciton formation and ignore the electron-hole exchange interaction. The lattice Hamil-

tonian can be transformed into the momentum space with the Fourier transformation $(e_{\vec{k},\sigma}, h_{\vec{k},\sigma}) = 1/\sqrt{\Omega} \Sigma_i e^{i\vec{k}\cdot\vec{R}_i}(e_{i,\sigma}, h_{i,\sigma})$. The result reads

$$\mathcal{H}_{kin}^{(p)}(\vec{k}) = \sum_{\vec{k},\sigma,\sigma',p} [(\zeta_{\vec{k}}^{(p)} - \mu_p)\delta_{\sigma,\sigma'} + V_p \tau_p (s_z)_{\sigma,\sigma'}] p_{\vec{k},\sigma}^\dagger p_{\vec{k},\sigma'},$$

$$\mathcal{H}_R^{(e)}(\vec{k}) = \sum_{\vec{k}} i\alpha(\sin k_x - i\sin k_y) e_{\vec{k}\uparrow}^\dagger e_{\vec{k}\downarrow} + \text{H.c.},$$

$$\mathcal{H}_R^{(h)}(\vec{k}) = \sum_{\vec{k}} i\beta(a_k - ib_k) h_{\vec{k}\Uparrow}^\dagger h_{\vec{k}\Downarrow} + \text{H.c.},$$

$$\mathcal{H}_{int}^{(e-h)} = -\frac{1}{2\Omega}\sum_{\vec{k},\vec{k}',\vec{q},\sigma,\sigma'} U^{(eh)}(q) e_{\vec{k}+\vec{q}\sigma}^\dagger h_{\vec{k}'-\vec{q}\sigma'}^\dagger h_{\vec{k}'\sigma'} e_{\vec{k}\sigma}, \quad (2)$$

where $U^{(eh)}(q) = \frac{2\pi e^2}{\epsilon q} e^{-qd}$, $\zeta_{\vec{k}}^{(p)} = -2t_p(\cos k_x + \cos k_y)$, $a_k = 2(3\cos k_y \sin k_x - \sin k_x \cos k_x - 2\sin k_x)$, and $b_k = 2(-3\cos k_x \sin k_y + \sin k_y \cos k_y + 2\sin k_y)$. In the above Hamiltonian, the interlayer tunneling is neglected because the insulating spacer can supply a high barrier to stop the direct interlayer hopping. We also neglect the intralayer electron-electron and hole-hole interactions since they are expected to renormalize the single-particle energy of each layer and have no essential influence on the topological properties of the system. In the mean-field approximation, the above Hamiltonian can be written as

$$\mathcal{H}_{MF} = \sum_{\vec{k},\sigma,\sigma',p} [(\zeta_{\vec{k}}^{(p)} - \mu_p)\delta_{\sigma,\sigma'} + V_p \tau_p (s_z)_{\sigma,\sigma'}] p_{\vec{k},\sigma}^\dagger p_{\vec{k},\sigma'}$$

$$+ \sum_p \mathcal{H}_R^{(p)} - \frac{1}{2}\sum_{\vec{k}\sigma\sigma'} [\Delta_{\sigma\sigma'}(\vec{k}) e_{\vec{k}\sigma}^\dagger h_{-\vec{k}\sigma'}^\dagger + \text{H.c.}]$$

$$+ \frac{1}{2\Omega}\sum_{\vec{k}\vec{q}\sigma\sigma'} \frac{\Delta_{\sigma\sigma'}(\vec{k})\Delta_{\sigma\sigma'}^*(\vec{k}-\vec{q})}{U^{(eh)}(q)}, \quad (3)$$

where the EOPs are defined as

$$\Delta_{\sigma\sigma'}(\vec{k}) = \frac{1}{\Omega}\sum_{\vec{q}} U^{(eh)}(q) \langle h_{-\vec{k}+\vec{q}\sigma'} e_{\vec{k}-\vec{q}\sigma} \rangle. \quad (4)$$

In the Nambu notation with combined e-h field operator basis $\psi = [e_{\vec{k}\uparrow} e_{\vec{k}\downarrow} h_{-\vec{k}\Uparrow}^\dagger h_{-\vec{k}\Downarrow}^\dagger]^T$, the mean-field Hamiltonian is expressed as $\mathcal{H}_{MF} = \psi^\dagger H_{MF} \psi + \text{const}$ with

$$H_{MF} = \begin{bmatrix} \mathbf{\Sigma}_{\vec{k}}^{(e)} - \mu_e + V_e s_z & \mathbf{\Delta}(\vec{k}) \\ \mathbf{\Delta}^\dagger(\vec{k}) & \mathbf{\Sigma}_{-\vec{k}}^{(h)} + \mu_h + V_h s_z \end{bmatrix}, \quad (5)$$

where $\mathbf{\Sigma}_{\pm\vec{k}}^{(p)} = \pm \zeta_{\pm\vec{k}}^{(p)} I \pm \mathcal{H}_R^{(p)}(\pm\vec{k})$ and

$$\mathbf{\Delta}(\vec{k}) = -\frac{1}{2}\begin{bmatrix} \Delta_{\uparrow\Uparrow}(\vec{k}) & \Delta_{\uparrow\Downarrow}(\vec{k}) \\ \Delta_{\downarrow\Uparrow}(\vec{k}) & \Delta_{\downarrow\Downarrow}(\vec{k}) \end{bmatrix} \quad (6)$$

with $\Delta_{\sigma\sigma'}(\vec{k})$ defined in Eq. (4).

The complex EOPs $\Delta_{\sigma\sigma'}(\vec{k})$ can be self-consistently obtained from exact numerical calculation of Eqs. (3) and (4) with respect to minimizing the ground-state energy. In our
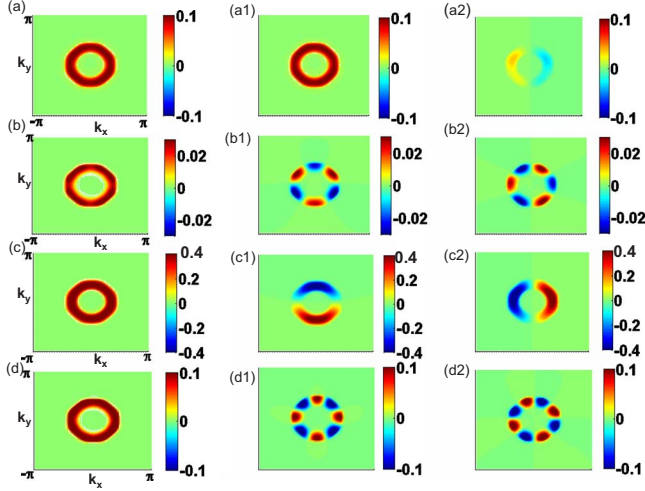
FIG. 2. (Color online) The left (middle, right) panels, respectively, show our calculated magnitudes (real parts, imaginary parts) of the EOPs $\Delta_{\uparrow\Uparrow}(\vec{k})$, $\Delta_{\uparrow\Downarrow}(\vec{k})$, $\Delta_{\downarrow\Uparrow}(\vec{k})$, and $\Delta_{\downarrow\Downarrow}(\vec{k})$, at a typical setup of magnetization parameters $(V_e, V_h) = (1, 1)$.

numerical calculation of $\Delta_{\sigma\sigma'}(\vec{k})$, we set the lattice size 81×81 and take $t_e = t_h = 1$, $\mu_e = \mu_h = -4$, $\alpha = 0.5$, and $\beta = 0.5$. There are four different kinds of choices for the perpendicular magnetization in the two magnetic films adjacent to the bilayer system. For the parallel configurations, in our numerical simulations we choose $(V_e, V_h) = (1, 1)$ and $(V_e, V_h) = (-1, -1)$ while for the antiparallel configurations we choose $(V_e, V_h) = (-1, 1)$ and $(V_e, V_h) = (1, -1)$. From our extensive numerical results, we find that only one spin channel of EOPs is dominated for each of the four choices of (V_e, V_h). Furthermore, we find that the EOPs will obtain k-dependent phases due to the Rashba SO coupling. For convenience of discussion, we define $\chi_k = \arctan(\sin k_y / \sin k_x)$ and $\tau_k = \arctan(b_k / a_k)$. As a typical example, the numerical results of EOPs for $(V_e, V_h) = (1, 1)$ are shown in Fig. 2. In this case, one can find from Fig. 2 that the component $\Delta_{\downarrow\Uparrow}(\vec{k})$ in EOP matrix Eq. (6) is dominant while the amplitudes of the other three components $(\Delta_{\uparrow\Uparrow}, \Delta_{\uparrow\Downarrow}, \Delta_{\downarrow\Downarrow})$ are negligibly small. With keeping in mind that the k-dependent phases of EOPs are obviously due to the Rashba SO interaction, we have analytically constructed various possible SO interaction-induced phases in EOPs and turned to compare these analytic approximate expressions with our exact numerical results. Table I summarizes the most optimal approximate phases for the four magnetic configurations. As an illustration, we plot

TABLE I. Dominant spin channel and approximate analytical EOP phase factors for different magnetization configurations.

(V_e, V_h)	Dominant EOP component	Phases of $(\Delta_{\uparrow\Uparrow}, \Delta_{\uparrow\Downarrow}, \Delta_{\downarrow\Uparrow}, \Delta_{\downarrow\Downarrow})$
$(1,1)$	$\Delta_{\downarrow\Uparrow}(\vec{k})$	$(1, -ie^{i\tau_k}, ie^{i\chi_k}, e^{i(\chi_k + \tau_k)})$
$(-1,1)$	$\Delta_{\uparrow\Uparrow}(\vec{k})$	$(ie^{-i\chi_k}, e^{-i\chi_k + i\tau_k}, -1, ie^{i\tau_k})$
$(-1,-1)$	$\Delta_{\uparrow\Downarrow}(\vec{k})$	$(e^{-i(\chi_k + \tau_k)}, -ie^{-i\chi_k}, ie^{-i\tau_k}, 1)$
$(1,-1)$	$\Delta_{\downarrow\Downarrow}(\vec{k})$	$(-ie^{i\tau_k}, -1, e^{i\chi_k - i\tau_k}, -ie^{i\chi_k})$

in Fig. 3 our derived approximate condensate phases for the case of $(V_e, V_h) = (1, 1)$ and compare them with the exact numerical result shown in Fig. 2. The agreement is clear. Note that usually, in semiconductor materials the electron effective mass m_e near the bottom of the conduction band is different from the heavy-hole effective mass m_h near the top of the valence band and we know that t_p is proportional to the $1/m_p$. Hence, generally, t_e is not equal to t_h. For a more realistic case, we have set $t_e = 1.0$ and $t_h = 0.5$ with unchanged $|V_e| = |V_h| = 1$. Thanks to the fact that α and β can be influenced by doping, gated voltages, material of quantum wells, etc., we can assume $\alpha = 0.5$ and $\beta = 0.25$. Then, we have found that $\mu_e = -4.0$ and $\mu_h = -2.45$ can also give the nearly identical Fermi surfaces of the electron and heavy hole. This guaranteed Fermi-surface nesting enables our conclusions in this paper to be valid in a wide range of realistic parameter regime. For simpleness of discussion, we assumed the parameter values $t_e = t_h = 1.0$.

With the help of Table I, we expect that the k-dependent phases in the EOPs may lead to the nontrivially chiral topological orders. For instance, let us consider the case of $(V_e, V_h) = (1, 1)$. In the continuum limit, $e^{i\chi_k} \sim \frac{k_x + ik_y}{k}$, and thus $\Delta_{\downarrow\Uparrow}(\vec{k}) \sim i|\Delta_{\downarrow\Uparrow}(\vec{k})|\frac{k_x + ik_y}{k}$. That means the $(p_x + ip_y)$-like pairing emerges.

Moreover, an explicit picture of chiral TEI can be well understood in the two-band approximation. To reveal this fact, first the noninteracting part in the total Hamiltonian is rewritten in the single-particle eigenstate space as

$$\mathcal{H}_0 = \sum_{\vec{k},s} E_{es}(\vec{k})\psi_{es}^\dagger(\vec{k})\psi_{es}(\vec{k}) + E_{hs}(\vec{k})\psi_{hs}(-\vec{k})\psi_{hs}^\dagger(-\vec{k}), \quad (7)$$

where $E_{es} = \zeta_{\vec{k}}^{(e)} - \mu_e + s\sqrt{\alpha^2(\sin^2 k_x + \sin^2 k_y) + V_e^2}$ and $E_{hs} = -\zeta_{-\vec{k}}^{(h)} + \mu_h + s\sqrt{\beta^2(a_k^2 + b_k^2) + V_h^2} (s = +, -)$ are, respectively, electron and heavy-hole band energies, and ψ_{ps} denotes the relevant annihilation field operators. Here the single-particle eigenstates are given by

$$\varphi_{e-}(\vec{k}) = e^{i\theta_k} - [if_+(k)e^{-i\chi_k}, f_-(k), 0, 0]^T,$$

$$\varphi_{e+}(\vec{k}) = e^{i\theta_k}[f_-(k), -if_+(k)e^{i\chi_k}, 0, 0]^T,$$

$$\varphi_{h-}(\vec{k}) = e^{i\vartheta_k}[0, 0, ig_+(k)e^{i\tau_k}, g_-(k)]^T,$$

$$\varphi_{h+}(\vec{k}) = e^{i\vartheta_k}[0, 0, g_-(k), ig_+(k)e^{-i\tau_k}]^T, \quad (8)$$

where

$$f_\pm(k) = \frac{\alpha\sqrt{\sin^2 k_x + \sin^2 k_y}}{\sqrt{\alpha^2(\sin^2 k_x + \sin^2 k_y) + [\sqrt{\alpha^2(\sin^2 k_x + \sin^2 k_y) + V_e^2} \pm V_e]^2}}$$

and

$$g_\pm(k) = \frac{\beta\sqrt{a_k^2 + b_k^2}}{\sqrt{\beta^2(a_k^2 + b_k^2) + [\sqrt{\beta^2(a_k^2 + b_k^2) + V_h^2} \pm V_h]^2}}.$$

Note that θ_k and ϑ_k are k-dependent phases and are in principal determined, during exciton formation, by exactly solving the ground state of the system through our above self-consistent calculation. The single-particle bands $E_{p\pm}(\vec{k})$ are
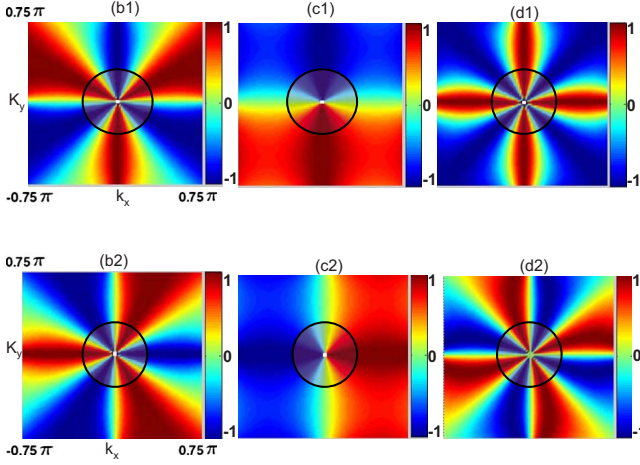
FIG. 3. (Color online) (From left to right) Phases factors of the EOPs $\Delta_{\uparrow\Downarrow}(\vec{k})$, $\Delta_{\downarrow\Uparrow}(\vec{k})$, and $\Delta_{\downarrow\Downarrow}(\vec{k})$ that are listed in Table I with $(V_e, V_h) = (1, 1)$. The imaginary part of the component $\Delta_{\uparrow\Uparrow}(\vec{k})$ is negligibly small [see Fig. 2(a) and 2]. Here the upper and lower panels, respectively, plot the real and imaginary parts of these three phase factors. The black cirques denote Fermi surface.

shown in Fig. 1(b) (solid curves), from which it is easy to find that the excitons are preferably formed between the lower electron band E_{e-} and the upper hole band E_{h+}. Moreover, the pairing relates to the Fermi surface of the bilayer system. With the values of the tunable parameters shown in the caption of the Fig. 1, the band E_{e-} and band E_{h+} have the nearly perfect nesting Fermi surface with the Fermi energy E_F being nearly zero, (namely, $\mu_p = -4t_p$). Hence, we can deal with pairing in BCS picture in this situation. Now, we consider the electron-hole interaction part in Eq. (2) in terms of the filled electron band E_{e-} and hole band E_{h+}. In order to obtain an explicit picture, we use a rough approximation by assuming a short-range interaction potential $U^{(eh)}(q) = U\delta(q)$. Then, after mean-field treatment, the resultant two-band Hamiltonian for our exciton system is given by

$$\bar{H}_{MF} \approx \sum_{\vec{k}} E_{e-}(\vec{k})\psi_{e-}^{\dagger}(\vec{k})\psi_{e-}(\vec{k}) + \sum_{\vec{k}} E_{h+}(\vec{k})\psi_{h+}(-\vec{k})\psi_{h+}^{\dagger}(-\vec{k})$$

$$- \frac{1}{2}\sum_{\vec{k}} [\bar{\Delta}(\vec{k})\psi_{e-}^{\dagger}(\vec{k})\psi_{h+}^{\dagger}(-\vec{k}) + \text{H.c.}] + \frac{1}{2}\sum_{\vec{k}} \frac{|\bar{\Delta}(\vec{k})|^2}{U},$$
(9)

where $\bar{\Delta}(\vec{k}) = \sum_{s,s'} Uf_s^2(k)g_{s'}^2(k)\langle\psi_{h+}(-\vec{k})\psi_{e-}(\vec{k})\rangle$. $(s, s' = \pm)$ The straightforward calculation can prove

$$\sum_{s,s'} f_s^2(k)g_{s'}^2(k) \sim 1$$

near the Fermi wave vector k_F. So $\bar{\Delta}(\vec{k}) \approx \Delta_0$ is almost k independent and only nonzero around k_F in BCS-type picture. In practice we can introduce a factor $\gamma(\vec{k}) = e^{-c(k-k_F)^2}e^{i\omega}$ (c and ω are real constants) to fit our exact multiband self-consistent numerical results (say, Fig. 2) in the whole Brillouin zone (BZ). The gaped energy spectrum

of $\bar{H}_{MF}$ is shown in Fig. 1(b) (dashed lines). Now, in the two-band approximation, the EOPs in Eq. (6) have the expressions as follows:

$$\mathbf{\Delta}(\vec{k}) = \frac{\Delta_0\gamma(\vec{k})e^{i(\theta_k - \vartheta_k)}}{2}$$

$$\times \begin{bmatrix} if_+(k)g_-(k)e^{-i\chi_k} & f_+(k)g_+(k)e^{-i\chi_k + i\tau_k} \\ -f_-(k)g_-(k) & if_-(k)g_+(k)e^{i\tau_k} \end{bmatrix}, \quad (10)$$

where the phases $e^{i(\theta_k - \vartheta_k + \omega)}$ are confirmed through our self-consistent calculation. It turns out that Eq. (10) gives a nice description of the numerical results.

III. CHIRAL TOPOLOGICAL ORDER

In the presence of exchange fields (V_e, V_h) induced by the ferromagnetic films, the TRS of the system is broken. No less than the AQHE, the nonzero TKNN number can undoubtedly characterize the topological nature of the system if a stable bulk gap separates the ground state and excited states. That means the topological property of the system will not be changed without bulk gap closing in spite of adiabatically deforming $|\Delta_{\sigma\sigma'}(\vec{k})|$ at the given exchange fields. Hence, $\gamma(\vec{k})$ in Eq. (10) is inessential for the system's topological property. Moreover, only the dominant component of EOPs decides the system's topological property at the given (V_e, V_h). The straightforward calculation of I_{TKNN} in Eq. (11) can prove the above two arguments.

In the following discussion, we use Eq. (10) to consider the system's topological properties. In general, in the spin-dependent Nambu space $(e_{\vec{k}\uparrow}e_{\vec{k}\downarrow}h_{-\vec{k}\Uparrow}^{\dagger}h_{-\vec{k}\Downarrow}^{\dagger})$, the EOPs in different spin channels are affected by the effective exchange fields. Additionally, the strong Rashba SO interaction flaws the spin polarization of the carries along the z direction. The total effect leads the factors $f_{\pm}(k)g_{\pm}(k)$ to emerge in different spin channels of EOPs and which decide the dominant one at given (V_e, V_h). For convenience of the following discussion, we use $(\Delta_0^{uu}, \Delta_0^{ud}, \Delta_0^{du}, \Delta_0^{dd})$ to denote $\Delta_0[f_+(k)g_-(k), f_+(k)g_+(k), f_-(k)g_-(k), f_-(k)g_+(k)]$. The topological nature of the ground state can be characterized by nonzero I_{TKNN}, which reads

$$I_{\text{TKNN}} = \sum_{n=1,2} C_n$$

$$= -\frac{1}{2\pi}\sum_{n=1,2}\int_{\text{BZ}} d^2k\,\Omega_n(\vec{k}), \quad (11)$$

where C_n is the Chern number for the nth mean-field energy band calculated via the Berry curvature $\Omega_n(\vec{k}) = -2\,\text{Im}\langle\frac{\partial u_n}{\partial k_x}|\frac{\partial u_n}{\partial k_y}\rangle$. Here $|u_n\rangle$ is the eigenstate of the mean-field Hamiltonian of Eq. (5) with $\mathbf{\Delta}(\vec{k})$ being the form of Eq. (10). The general analytic process is too complicated. If we consider one special case for $(V_e, V_h) = (1, 1)$ with $\Delta_{\downarrow\Uparrow} = i\Delta_0 e^{i\chi_k}/2$ and $\Delta_{\uparrow\Uparrow} = \Delta_{\uparrow\Downarrow} = \Delta_{\downarrow\Downarrow} = 0$, the specific forms of $|u_n\rangle$ are that $|u_1\rangle = [1, 0, 0, 0]^T$ and $|u_2\rangle = [0, -i\sqrt{1+A(\vec{k})}e^{i\chi_k}, \sqrt{1-A(\vec{k})}, 0]^T$ in the basis of energy bands, where

TABLE II. The TKNN numbers for effective exchange fields and corresponding EOP amplitudes.

(V_e, V_h)	Δ_0	$(\Delta_0^{uu}, \Delta_0^{ud}, \Delta_0^{du}, \Delta_0^{dd})$	I_{TKNN}
$(1,1)$	0.5	0.5(0,0,1,0)	1
$(-1,1)$	0.5	0.5(1,0,0,0)	-1
$(-1,-1)$	0.5	0.5(0,1,0,0)	-1
$(1,-1)$	0.5	0.5(0,0,0,1)	1

$$A(\vec{k}) = \frac{E_{h+}(\vec{k}) - E_{e-}(\vec{k})}{\sqrt{[E_{h+}(\vec{k}) - E_{e-}(\vec{k})]^2 + \Delta_0^2}}.$$

The straightforward calculation of Eq. (11) can give I_{TKNN}. For definiteness, we give the numerical calculations for general cases and summarize the results in Table II, which clearly shows chiral topological order with its winding behavior depending on the choice of exchange-field parameters. From the bulk-edge correspondence, the nontrivial bulk topological number implies gapless edge states in the system with finite size.

In order to confirm the existence of the gapless edge states, we assume that the square-lattice system has two edges in y direction and is boundless in x direction. Correspondingly, we choose open boundary condition in y direction and periodic boundary condition in x direction of the lattice Hamiltonian in Eq. (1) in mean-field approximation. The calculated energy spectrum at a typical case of $(V_e, V_h) = (1,1)$ is illustrated in Fig. 4(a). The red-solid and blue-dashed lines correspond to the different edge states with contrary chirality. It is easy to find that the number of the gapless edge states is consistent with the bulk theory characterized by I_{TKNN}.

IV. TRANSPORT PROPERTY OF EDGE STATES

The nontrivial transport phenomena can be predicted due to the emergence of the edge states in our system. From Fig. 4(a), we can find that the edge sates in different chiral topological order propagate on each boundary with opposite velocities and can be described by the following Hamiltonian:

$$H_{edge}^{\rho} = \pm \sum_{k_x \geq 0} \lambda_{\rho} v_F k_x \eta_{\rho}^{\dagger}(k_x, y) \eta_{\rho}(k_x, y), \qquad (12)$$

where $\pm$ represents different edges and $\eta = 1, \ldots, 4$ labels four different kinds of magnetic configurations, namely, $\lambda_1 = \lambda_4 = 1$ and $\lambda_2 = \lambda_3 = -1$, v_F is the Fermi velocity and k_x is the momentum measured from the Fermi surface. The quasiparticle operators for case $(V_e, V_h) = (1,1)$ read

$$\eta_1(k_x, y)$$
$$= u_1(k_x, y) e_{\uparrow}(y) + v_1(k_x, y) h_{\Uparrow}^{\dagger}(y). \qquad (13)$$

The other cases have the similar forms. Due to the missing of the PHS, the quasiparticles are not Majorana fermions.

The edge states in the AQHE systems can be usually detected through the Hall conductance responding to the
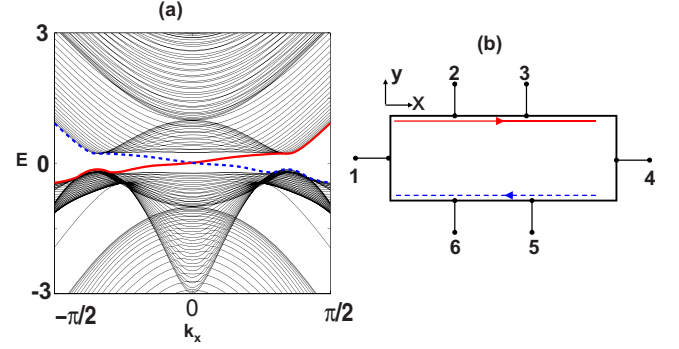

FIG. 4. (Color online) (a) The energy spectrum of the bilayer square-lattice system with two edges at the y direction. k_x denotes the momentum in the x direction. The magnetization parameters are set at $(V_e, V_h) = (1,1)$. The red-solid and blue-dashed lines denote the edge states locating on different edges. (b), Six-terminal Hall bar for detection of the edge states. The red-solid and blue-dashed lines with arrows represent the edge modes propagating in opposite direction.

external electromagnetic field.[16,17] However, the edge states in our system are excitons which are charge neutral. A simple approach is to use thermal transport measurement which is often used to judge the pair properties in high-T_c superconductors.[18,19] The six-terminal Hall bar showed in Fig. 4(b) for detecting the edge states of quantum (spin) Hall effect can be used to detect the thermal conductance. The same setup has been used by Sato *et al.*[20] to detect the edge state in topological superconductor. We give the similar considerations with that in Ref. 20 as follows. The temperature must be sufficiently lower than the exciton gap ($T \ll \Delta_0$) in order to suppress the contributions from the fermionic excitations (electrons and holes) in the bulk and bosonic (phonons) excitations. The thermal conductance is defined by $G(T) = I_{14}(T)/(\Delta T)_{14}$, where $I_{ij}(T)$ is a thermal current between contacts i and j, and $(\Delta T)_{ij}$ is the temperature difference between these contacts. In the low-temperature limit, the T dependence of $G(T)$ have three origins: the linear law $\propto T$ from edge states for phase η, the exponentially low $\sim e^{-\Delta_0/T}$ from bulk quasiparticles and the power law $\propto T^3$ from phonons. Furthermore, in analogy with the quantum spin Hall current discussed in Ref. 21, there is no temperature difference between contacts 2 and 3 (5 and 6) because the edge current is dissipationless.

V. DISCUSSION AND CONCLUSION

More recently, some proposals[20,22–24] have investigated the similar chiral topological order, for which the spin-orbit interaction and Zeeman field have also played an important role. Compared to those proposals, the excitonic insulator in the present paper is due to the attractive coulomb interaction between electrons and heavy holes, and the remarkable forms of the excitonic order parameters are confirmed with self-consistent calculations in our proposal.

In conclusion, we have presented a scheme to realize the chiral topological excitonic insulator in the double quantum wells adjacent to two ferromagnetic films. We have predicted

different topologically nontrivial orders emergent along with changes in the magnetization orientations in the ferromagnetic films. The topologically nontrivial orders can be characterized by the chiral topological numbers defined with TKNN numbers in bulk system or chiral edge states in edged system. Furthermore, we have given an experimental scheme to detect the excitonic gapless edge states.

*Corresponding author; zhang_ping@iapcm.ac.cn

[1] F. D. M. Haldane, Phys. Rev. Lett. **61**, 2015 (1988).

[2] D. J. Thouless, M. Kohmoto, M. P. Nightingale, and M. den Nijs, Phys. Rev. Lett. **49**, 405 (1982).

[3] B. I. Halperin, Phys. Rev. B **25**, 2185 (1982).

[4] Y. Hatsugai, Phys. Rev. Lett. **71**, 3697 (1993).

[5] C. X. Liu, X. L. Qi, X. Dai, Z. Fang, and S. C. Zhang, Phys. Rev. Lett. **101**, 146802 (2008).

[6] N. Read and D. Green, Phys. Rev. B **61**, 10267 (2000).

[7] J. Nitta, T. Akazaki, H. Takayanagi, and T. Enoki, Phys. Rev. Lett. **78**, 1335 (1997).

[8] J. P. Lu, J. B. Yau, S. P. Shukla, M. Shayegan, L. Wissinger, U. Rössler, and R. Winkler, Phys. Rev. Lett. **81**, 1282 (1998).

[9] D. Grundler, Phys. Rev. Lett. **84**, 6074 (2000).

[10] S. J. Papadakis, E. P. De Poortere, H. C. Manoharan, M. Shayegan, and R. Winkler, Science **283**, 2056 (1999).

[11] L. P. Gor'kov and E. I. Rashba, Phys. Rev. Lett. **87**, 037004 (2001).

[12] G. Engels, J. Lange, Th. Schäpers, and H. Lüth, Phys. Rev. B **55**, R1958 (1997).

[13] R. Winkler, Phys. Rev. B **62**, 4245 (2000).

[14] R. Winkler, H. Noh, E. Tutuc, and M. Shayegan, Phys. Rev. B **65**, 155303 (2002).

[15] C. L. Yang, H. T. He, L. Ding, L. J. Cui, Y. P. Zeng, J. N. Wang, and W. K. Ge, Phys. Rev. Lett. **96**, 186605 (2006).

[16] P. L. McEuen, A. Szafer, C. A. Richter, B. W. Alphenaar, J. K. Jain, A. D. Stone, R. G. Wheeler, and R. N. Sacks, Phys. Rev. Lett. **64**, 2062 (1990).

[17] J. K. Wang and V. J. Goldman, Phys. Rev. Lett. **67**, 749 (1991).

[18] R. W. Hill, C. Proust, L. Taillefer, P. Fournier, and R. L. Greene, Nature (London) **414**, 711 (2001).

[19] M. F. Smith, J. Paglione, M. B. Walker, and L. Taillefer, Phys. Rev. B **71**, 014506 (2005).

[20] M. Sato and S. Fujimoto, Phys. Rev. B **79**, 094504 (2009).

[21] B. A. Bernevig, T. L. Hughes, and S. C. Zhang, Science **314**, 1757 (2006).

[22] M. Sato, Y. Takahashi, and S. Fujimoto, Phys. Rev. Lett. **103**, 020401 (2009).

[23] J. D. Sau, R. M. Lutchyn, S. Tewari, and S. Das Sarma, Phys. Rev. Lett. **104**, 040502 (2010).

[24] J. Alicea, Phys. Rev. B **81**, 125318 (2010).